

A semi-classical analysis of Dirac fermions in 2+1 dimensions

Moitri Maiti and R. Shankar

The Institute of Mathematical Sciences, C.I.T Campus, Taramani,
Chennai-600113, India.

E-mail: moitri@imsc.res.in, shankar@imsc.res.in

Abstract.

We investigate the semiclassical dynamics of massless Dirac fermions in 2+1 dimensions in the presence of external electromagnetic fields. By generalizing the α matrices by two generators of the $SU(2)$ group in the $(2S+1)$ dimensional representation and doing a certain scaling, we formulate a $S \rightarrow \infty$ limit where the orbital and the spinor degrees become classical. We solve for the classical trajectories for a free particle on a cylinder and a particle in a constant magnetic field. We compare the semiclassical spectrum, obtained by Bohr-Sommerfeld quantization with the exact quantum spectrum for low values of S . For the free particle, the semiclassical spectrum is exact. For the particle in a constant magnetic field, the semiclassical spectrum reproduces all the qualitative features of the exact quantum spectrum at all S . The quantitative fit for $S = 1/2$ is reasonably good.

PACS numbers: 73.22.-f, 73.22.Pr, 03.65.Sq

1. Introduction

The recent developments in discovery of graphene [1] and topological insulators [2] has aroused interest in the physics of Dirac fermions in two and three spatial dimensions. In device applications, it is often necessary to consider the system in the presence of external, spatially varying fields [3, 4]. While the Dirac equation generally can be solved numerically in these cases, the semiclassical limit of a quantum system often provides useful physical insights into the dynamics. Another interesting aspect of Dirac fermions is the strong coupling between orbital and spinor dynamics leading to the well known phenomenon of *Zitterbewegung*. This effect in solid-state systems, in particular graphene, has been a topic of recent interest [5, 6, 7].

The 2+1 dimensional Dirac equation can be looked upon as the analogue of the physical 3+1 dimensional Dirac equation. The Hilbert space of Dirac spinors are then projective unitary irreducible representations of the 2+1 Lorentz group [8]. In the condensed matter context mentioned above, there is no Lorentz invariance. The Dirac equation is valid only in a special frame, namely the rest frame of the material. The physical significance of the two components of the Dirac spinor depends on the details of the material as we describe below for graphene and topological insulators.

The Dirac equation which describes the charge carriers in graphene is a consequence of graphene's honeycomb lattice crystal structure which consists of two

inequivalent triangular sublattices. The two bands arise due to the hopping between the two sublattices and touch each other at two points, the so called K and K' points of the Brillouin zone. The energy dispersion is linear near these two points. The dynamics of the low energy quasi-particles and quasi-holes are effectively described by the massless 2+1 dimensional Dirac equation with the role of c played by the Fermi velocity v_F . There are two species of Dirac fermions, one corresponding to the excitations near the K point and the other near the K' point. For each of these, the two components of the Dirac spinor represent the probability amplitudes at the two sublattices. While the electrons in graphene are confined to two dimensions, they have a physical spin degree of freedom. This manifests in the effective Dirac theory as an internal degree of freedom. There are thus a total of four species of Dirac fermions in graphene.

The 2+1 dimensional Dirac equation also describes the low energy quasi-particles at the surface of 3-dimensional topological insulators [9]. Examples of 3-dimensional topological insulators include Bi_2Se_3 , Bi_2Te_3 , Sb_2Te_3 . While in graphene the Dirac equation arises from the honeycomb lattice structure, in topological insulators it comes from the strong spin-orbit coupling. Thus unlike graphene where the two components of the Dirac spinor represent the wave functions on the two sublattices, in topological insulators they represent the wave functions of the two spin projections.

The earliest approach towards semiclassical analysis of a Dirac particle in an electromagnetic field was by W.Pauli[10]. He determined the phase of a WKB spinor for relativistic point particles for some special cases and argued that in the semi-classical limit, the translational motion is independent of the spin-degree of freedom. This conclusion was criticized by de Broglie[11] with the remark that electromagnetic moments are expected to influence the trajectories in the semi-classical limit. The issue was latter addressed and clarified by Rubinow and Keller[12]. They pointed out that the moments of an electron are proportional to \hbar so that in leading order as $\hbar \rightarrow 0$ the influence of the spin of the particle on the trajectories vanishes. Thus in a formalism when the spin is also taken to be large we can expect it to couple to the orbital dynamics. We analyze such a formalism in this paper.

In their study of multi-component wavefunction Yabana and Horiuchi [13] pointed out the necessity of including the geometric phase in the Bohr-Sommerfeld quantization condition. However in their approach and many of the previous approaches to the semi-classical analysis of systems with many component wave functions, [14, 15, 16] the spin and orbital degrees of freedom are treated on a different footing, with the orbital degree of freedom being treated semi-classically and spin quantum mechanically. The orbital and spin degrees of freedom were combined together for the first time by Pletyukhov *et. al*[18] in a joint (extended) phase space where the description of a spin by continuous variables is achieved by using the basis of coherent states. The partition function for a system with spin-orbit coupling is then written in the path integral representation using coherent states. The semi-classical propagator or trace formula is evaluated for the system applying stationary phase approximation[17].

In this paper we follow the extended phase space approach and present a systematic formalism for the semi-classical analysis for the massless Dirac fermion in 2+1 dimensions in presence of external electromagnetic fields. We use the fact that, in 2+1 dimensions, the 3 Dirac matrices are elements of the two dimensional representation of the $SU(2)$ algebra to generalise them to be the corresponding elements in the $2S+1$ dimensional algebra. We then establish, using the path integral

formalism that there is a systematic stationary phase approximation with $1/S$ being the small parameter. The classical equations of motion couples orbital and the spinor degrees of freedom. For cases of free particle on a cylinder and particle in a constant magnetic field closed orbit solutions are found and quantized using Bohr-Sommerfeld quantization. The classical solutions for the free particle are oscillatory rather than straight lines thus illustrating the phenomenon of *zitterbewegung*. Comparison with the exact quantum mechanical results shows that all the qualitative features of the spectrum are reproduced by the semi-classical analysis. The quantitative agreement is good even for small values of S , in particular $S = \frac{1}{2}$.

The organization of the rest of this paper is as follows. In section 2, we give the formulation of the path integral description of the propagator using coherent states and formulate a systematic semiclassical expansion in $1/S$. We write down the classical equations of motion and the quantization condition for the closed classical orbits. In section 3, the Dirac fermion on a cylinder in absence of any external field is studied. The particle in a constant external magnetic field is studied in section 4. The semi-classical and exact spectrum are compared in section 5. The results are summarized in section 6.

2. The Semi-Classical Expansion

We begin by outlining the general formalism to analyze the spectrum semi-classically. The hamiltonian for a single massless $S = \frac{1}{2}$ Dirac particle in 2 spatial dimensions, in the presence of external magnetic and spatially varying fields $V(\mathbf{x})$ is given by:

$$\mathcal{H} = v_F \alpha \cdot \Pi + eV(\mathbf{x}) \quad (2.1)$$

where, $\Pi_i = p_i - eA_i$ is the mechanical momentum, v_F is the Fermi velocity. The α matrices can be represented by the Pauli matrices and the wavefunctions by a two component spinor.

The hamiltonian in eqn.[2.1] is generalized by replacing the α^x and α^y matrices by two of the generators of the $SU(2)$ group in the $(2S+1)$ dimensional representation and written as:

$$\mathcal{H} = \frac{v_F}{S} \mathbf{S} \cdot \mathbf{\Pi} + eV(\mathbf{x}) \quad (2.2)$$

We note that while the system is rotationally invariant at all S , it is not Lorentz invariant for $S \neq 1/2$. We will explicitly see the consequences of this in the spectrum in later sections. However for applications to condensed matter systems, Lorentz invariance is not crucial. We resort to a path integral formalism to describe the time evolution of the system and find a systematic semiclassical parameter S for the combined orbital and spinor degree of freedom as described below.

The path integral is constructed using coherent state representation. The coherent states which describe the system are direct product of the usual phase-space coherent states $|\vec{x}, \vec{p}\rangle$ and $SU(2)$ -coherent states $|\vec{n}, \mu\rangle$ i.e

$$|\vec{x}, \vec{p}; \vec{n}, \mu\rangle = |\vec{x}, \vec{p}\rangle \otimes |\vec{n}, \mu\rangle \quad (2.3)$$

where $\vec{n} \cdot \vec{n} + \mu^2 = 1$.

The path integral representation of time evolution of the system from time t_i to time

t_f is:

$$\langle \vec{x}_f, \vec{p}_f; \vec{n}_f, \mu_f | e^{-\frac{i/\hbar \mathcal{H}(t_i - t_f)}{\hbar}} | \vec{x}_i, \vec{p}_i; \vec{n}_i, \mu_i \rangle = \int \mathcal{D}[\vec{n}(\tau, \zeta)] \mathcal{D}[\mu(\tau, \zeta)] \mathcal{D}[\vec{x}(t)] \mathcal{D}[\vec{p}(t)] e^{-\frac{i\mathcal{S}}{\hbar}} \quad (2.4)$$

$$\mathcal{S}[x(\vec{t}); p(\vec{t}); \vec{n}(\tau, \zeta), \mu(\tau, \zeta)] = \int_{t_i}^{t_f} dt (\vec{p} \cdot \frac{d\vec{x}}{dt} - \mathcal{H}) - \hbar S \Omega[\vec{n}(\tau, \zeta), \mu(\tau, \zeta)] \quad (2.5)$$

where \mathcal{S} is the action with:

$$\vec{x}(t_i) = \vec{x}_i; \quad \vec{p}(t_i) = \vec{p}_i; \quad \vec{n}(t_i) = \vec{n}_i; \quad \mu(t_i) = \mu_i \quad (2.6)$$

$$\vec{x}(t_f) = \vec{x}_f; \quad \vec{p}(t_f) = \vec{p}_f; \quad \vec{n}(t_f) = \vec{n}_f; \quad \mu(t_f) = \mu_f \quad (2.7)$$

$\Omega[\vec{n}(\tau, \zeta), \mu(\tau, \zeta)]$ is the geometric phase encompassed during time evolution and is written as:

$$\Omega[\vec{n}(\tau, \zeta), \mu(\tau, \zeta)] = \int_{\tau_i}^{\tau_f} d\tau \int_0^1 d\zeta \mu \epsilon_{ij} \partial_\tau n^i \partial_\zeta n^j, \quad i, j = 1, 2 \quad (2.8)$$

$\vec{n}(\tau; \zeta)$ parameterizes the surface on the unit sphere in 2 dimensions defined by the curve $\vec{n}(\tau)$, and the geodesics from $\vec{n}(\tau_i)$ and $\vec{n}(\tau_f)$ to the north pole (or some standard point on the unit sphere). For any arbitrary S it is convenient to write $\vec{S} = S\vec{n}$. The system variables are scaled in terms of the characteristic length scale λ and time scale ω of the system as:

$$\begin{aligned} x'_i &= \frac{x_i}{\lambda}, \quad p'_i = \frac{\lambda}{\hbar S} p_i, \quad t' = \omega t \\ A'_i &= \frac{e\lambda}{\hbar S} A_i, \quad \Pi'_i = \frac{\lambda}{\hbar S} \Pi_i, \quad V'(x'_i) = \frac{1}{e\omega\hbar S} V(x_i) \end{aligned} \quad (2.9)$$

Using Eqn.[2.9] the action \mathcal{S} can be written as:

$$\begin{aligned} &\mathcal{S}[x'(\vec{t}'); p'(\vec{t}'); \vec{n}(\tau, \zeta), \mu(\tau, \zeta)] \\ &= \hbar S \left[\int_{t_i}^{t_f} dt' (\vec{p}' \cdot \frac{d\vec{x}'}{dt'} - \mathbb{H}) - \Omega[\vec{n}(\tau, \zeta), \mu(\tau, \zeta)] \right] \end{aligned} \quad (2.10)$$

where,

$$\mathbb{H} = \vec{n} \cdot \Pi' + V'(x') \quad (2.11)$$

Henceforth we will drop the subscript in the variables keeping in mind that they are scaled and hence are dimensionless. The propagator in eqn.(2.4) can then be evaluated by a systematic stationary phase approximation with $1/S$ as the expansion parameter. In this paper we will find closed orbit solutions to the classical equations of motion and quantize them using the Bohr-Sommerfeld quantization procedure.

In the classical limit the system observables satisfy the following Poisson bracket relations:

$$\{x_i, p_j\} = \delta_{ij}; \quad \{n_i, n_j\} = \epsilon_{ij}\mu; \quad \{\mu, n_i\} = \epsilon_{ji}n_j \quad \{n_i, x_j\} = 0$$

and the equations of motion are:

$$\begin{aligned} \dot{x}_i &= p_i \\ \dot{\Pi}_i &= \epsilon_{ji}n_j - \partial_i V(x_i), \quad i = 1, 2 \\ \dot{n}_i &= \mu \epsilon_{ij}\Pi_j, \quad i, j = 1, 2 \\ \dot{\mu} &= \epsilon_{ij}n_i\Pi_j, \quad i, j = 1, 2 \end{aligned} \quad (2.12)$$

If the classical trajectories are closed then the action is quantized using Bohr-Sommerfeld quantization condition to find out the allowed orbits and subsequently quantize the spectrum. In terms of the canonical co-ordinate and the momentum, the quantization condition encloses an area in the phase space. For the Dirac particle in (2+1) dimensions, the quantization condition includes the contribution from geometric phase which is otherwise absent for quantization of Schrödinger particle, as follows:

$$\oint_C p_1 dx + \oint_C p_2 dy - \Omega[\vec{n}, \mu] = 2\pi \frac{m}{S}, \quad m = 0, 1, 2, \dots \quad (2.13)$$

where C denotes the closed orbits in the phase space. We use this method to analyze the spectrum for two solvable cases of (i) a free particle and (ii) a particle in a constant external magnetic field in following sections (3) and (4) and compare with the exact solutions.

3. Free Particle

3.1. Semi-classical expansion

Consider a massless Dirac particle on the surface of a cylinder of circumference L . In the absence of any spatially varying field $V(x)$ and magnetic field, the hamiltonian for the system is:

$$\mathbb{H}_{free} = \mathbf{n} \cdot \mathbf{p} \quad (3.1)$$

We take $\lambda = L$ and $\omega = \frac{v_F}{L}$. The action is:

$$\mathcal{S}[\vec{x}(t); \vec{p}(t); \vec{n}, \mu] = \hbar S \left[\int_{t_i}^{t_f} dt \left[p_x \frac{dx}{dt} - n_i p_i \right] - \Omega[\vec{n}, \mu] \right] \quad (3.2)$$

The equations of motion are as follows:

$$\begin{aligned} \dot{x}_i &= n_i, \quad i = 1, 2 \\ \dot{p}_i &= 0 \\ \dot{n}_i &= \mu \epsilon_{ij} p_j, \quad i, j = 1, 2 \\ \dot{\mu} &= \epsilon_{ij} n_i p_j, \quad i, j = 1, 2 \end{aligned} \quad (3.3)$$

We look into solutions for which $p(t) = p_x^0$, $p_y(t) = 0$ and the solutions are:

$$\begin{aligned} x(t) &= n_x^0 t + x_0 \\ y(t) &= \frac{1}{\omega} (\mu^0 \cos \omega t + n_y^0 \sin \omega t) \\ p(t) &= p_x^0 \\ n_x(t) &= n_x^0 \\ n_y(t) &= n_y^0 \cos \omega t - \mu^0 \sin \omega t \\ \mu(t) &= \mu^0 \cos \omega t + n_y^0 \sin \omega t \end{aligned} \quad (3.4)$$

where, $\omega = p_x^0$.

The velocity and hence the classical trajectories thus oscillate in the direction transverse to the momentum illustrating the phenomenon of *zitterbewegung*.

The geometrical phase traced out by the closed classical trajectories is:

$$\Omega = 2\pi(1 - \cos(\theta_0)) \quad (3.5)$$

where,

$$\cos(\theta_0) = \hat{n} \cdot \frac{\mathbf{p}_x^0 \hat{\mathbf{x}}}{\omega} = n_x^0 \quad (3.6)$$

From commensurate time-period for the linear motion and that for the orbital motion:

$$\frac{2\pi}{\omega} = \frac{1}{n_x^0} \quad (3.7)$$

The Bohr-Sommerfeld quantization condition following eqn.(2.13) for the free particle is:

$$\oint p_x^0 dx - 2\pi(1 - \cos \theta) = 2\pi \frac{m}{S} \quad (3.8)$$

where m is an integer. Substituting the value of $\cos \theta$ from (3.6), we have:

$$p_x^0 - 2\pi(1 - n_x^0) = 2\pi \frac{m}{S} \quad (3.9)$$

Quantizing each of the term individually, we get:

$$p_x^0 = 2\pi n/S \quad (3.10)$$

$$n_x^0 = (m_1/S + 1) \quad (3.11)$$

$$\text{where } n = 0, 1, 2, \dots, \quad -2S < m_1 < 0$$

The energy of the particle is given by:

$$\begin{aligned} E &= n_x p_x^0 \\ &= 2\pi n \left(\frac{m}{S}\right) \quad \text{where } m = -S, \dots, S \end{aligned} \quad (3.12)$$

Next we analyze the quantum mechanical spectrum of the free Dirac particle and compare with the spectrum obtained above.

3.2. Quantum spectrum

The hamiltonian in dimensionless units is given by:

$$\mathcal{H} = \frac{1}{S} \mathbf{S} \cdot \mathbf{p} \quad (3.13)$$

This hamiltonian can be easily diagonalised. To compare with the semiclassical spectrum, we consider plane waves propagating in the x direction. The periodic boundary conditions imply that $k_x = 2\pi n/L$. S_x has eigenvalues $m = -S, \dots, S$.

$$E = 2\pi n \frac{m}{S}, \quad n = 0, 1, 2, \dots \quad (3.14)$$

Comparing equations (3.12), (3.14) we find that the spectrum of the free particle obtained semi-classically is exactly identical to its quantum mechanical one.

Also note that the quantum spectrum consists of $2S + 1$ massless particles, travelling with speed mv_F . This illustrates our comment earlier that except at $S = 1/2$, the theory is not Lorentz invariant.

4. External magnetic field

4.1. Semi-classical quantization

In this section we study the massless Dirac particle in a constant magnetic field. The system is characterized by a length scale, the cyclotron radius l_c and a time scale, the cyclotron frequency ω_c which are:

$$l_c \equiv \sqrt{\frac{\hbar}{eB}} \quad \omega_c \equiv \frac{v_F}{l_c} \quad (4.1)$$

We choose $\lambda = l_c$ and $\omega = \omega_c$. The system variables are scaled in terms of the characteristic scales of the system following eqn.(2.9). The system is described by:

$$\mathbb{H}_{mag} = \mathbf{n} \cdot \mathbf{\Pi} \quad (4.2)$$

where $\mathbf{\Pi}$ related to the canonical momentum and the vector potential as $\Pi_i = p_i + A_i$. For a constant magnetic field, $\{\Pi_i, \Pi_j\} = \epsilon_{ij}$. We define another observable, the guiding center co-ordinate of the system $R_i \equiv x_i + \epsilon_{ij} \Pi_j$, which satisfies: $\{R_i, R_j\} = -\epsilon_{ij}$, $\{R_i, \Pi_j\} = 0$ & $\{R_i, n_j\} = 0$. It then follows that R_i are constants of motion,

$$\{R_i, \mathbb{H}_{mag}\} = 0, \quad i = 1, 2 \quad (4.3)$$

The canonical momentum p_i and the canonical co-ordinate x_i can be written in terms of the guiding center co-ordinate and the kinetic momentum as follows:

$$\begin{aligned} x &= R_x - \Pi_y; \quad y = R_y + \Pi_x \\ p_x &= (\Pi_x - R_y)/2; \quad p_y = (\Pi_y + R_x)/2 \end{aligned} \quad (4.4)$$

The equations of motion of the system in terms of \mathbf{R} , $\mathbf{\Pi}$, \mathbf{n} and μ can be written as:

$$\begin{aligned} \dot{R}_i &= 0 \\ \dot{\Pi}_i &= \epsilon_{ji} n_j \\ \dot{n}_i &= \mu \epsilon_{ij} \Pi_j, \quad i, j = 1, 2 \\ \dot{\mu} &= \epsilon_{ij} n_i \Pi_j, \quad i, j = 1, 2 \end{aligned} \quad (4.5)$$

We choose $R_i(t) = R_i$. Since R_i commutes with the hamiltonian it represents the infinite degeneracy of each Landau level in the exact solution. The system has rotation symmetry in the $x - y$ plane and for this closed system the angular momentum is conserved and is given as:

$$\frac{J_z}{S} = \epsilon_{ij} x_i p_j + \mu = \frac{1}{2} \Pi_i \Pi_i + \mu - \frac{1}{2} R_i R_i \quad (4.6)$$

in terms of the guiding center co-ordinate and the kinetic momentum.

The Bohr-Sommerfeld quantization condition in terms of Π and R_i is given as:

$$\frac{1}{2} \oint \left(\epsilon_{ij} \Pi_i \dot{\Pi}_j - \epsilon_{ij} R_i \dot{R}_j \right) dt - \Omega[\vec{n}, \mu] = 2\pi \frac{m}{S} \quad (4.7)$$

where $\Omega[n, \mu]$ is given by eqn.(3.5). To solve for $\mathbf{\Pi}$, \mathbf{n} and μ , we consider the following ansätze in which a) $\vec{n} \equiv n_x \hat{x} + n_y \hat{y}$ parallel to $\mathbf{\Pi}$. b) \vec{n} is perpendicular to the $\mathbf{\Pi}$. We look into each case separately in the following sections.

4.1.1. $\vec{n} \parallel \mathbf{\Pi}$ For this case, we consider $\mu = \cos(\theta)$. The components of $\mathbf{\Pi}$ are related to the *azimuthal* angle ϕ in the $x - y$ plane as:

$$\Pi_x = \Pi \cos \phi; \quad \Pi_y = \Pi \sin \phi \quad (4.8)$$

The equations of motion (4.5) in terms of ϕ and θ becomes:

$$\begin{aligned} \sin \theta \dot{\theta}(t) &= 0; \quad \cos \theta \dot{\theta}(t) = 0; \quad \dot{\Pi}(t) = 0 \\ \sin \theta \dot{\phi} &= -\cos \theta \Pi; \quad \Pi \dot{\phi}(t) = 2 \sin \theta \end{aligned} \quad (4.9)$$

and the solutions are:

$$\theta(t) = \theta_0 \quad (4.10)$$

$$\Pi(t) = \Pi_0 \quad (4.11)$$

$$\phi(t) = \sqrt{\cos(\theta_0)} \, t \quad (4.12)$$

where $\cos \theta_0 = \mu_0$. The corresponding trajectories are:

$$\begin{aligned} x(t) - R_x &= -\Pi_0 \sin \phi(t) \\ y(t) - R_y &= \Pi_0 \cos \phi(t) \end{aligned} \quad (4.13)$$

where Π_0 is related to θ_0 as:

$$\Pi_0^2 = -\frac{\sin^2 \theta_0}{\cos \theta_0}, \quad \pi/2 < \theta_0 < \pi \quad (4.14)$$

The particle trajectories are circular orbits centered around the guiding center.

For a given θ , the tip of the unit vector thus moves in closed orbits. The solid angle subtended by the closed path is given by eqn.(3.5). We then use the Bohr-Sommerfeld quantization rule to pick the allowed orbits. The quantization condition is:

$$\left(\frac{\Pi_0^2}{2} + \cos \theta_0 \right) = \frac{m'}{S} + 1, \quad (4.15)$$

where $m' = -2S, -2S+1, \dots$. With a change of variable $n = m' + 2S$, where n is an integer and little algebra we get,

$$\cos \theta_0 = \frac{1}{3} \left(\left(\frac{n}{S} - 1 \right) - \sqrt{\left(\frac{n}{S} - 1 \right)^2 + 3} \right) \quad (4.16)$$

from equations (4.14) and (4.15). The energy of the particle is given by:

$$E = \sin \theta_0 \Pi_0 = \pm \sin^2 \theta_0 \sqrt{\frac{1}{|\cos \theta_0|}}, \quad (4.17)$$

The angular momentum J_z for this class of solution is $\frac{J_z}{S} = \frac{\Pi_0^2}{2} + \cos \theta_0 - \frac{R_0^2}{2}$ which using the Bohr-Sommerfeld quantization condition eqn.(4.15),

$$\frac{J_z}{S} = \left(\frac{n}{S} - 1 \right) - \frac{R_0^2}{2} \quad (4.18)$$

where $R_0^2 = R_i R_i$. We demand $(J_z - S)$ to take integer values. This constraints $\frac{R_0^2}{2} = \frac{k}{S}$ where k is an integer. The quantum states corresponding to the different

values of k are degenerate, consistent with the infinite degeneracy of each Landau level.

For large n limit, $\cos \theta \sim \frac{1}{2n/S}$. The energy of the particle in this limit is:

$$E = \pm \sqrt{2n/S} \quad (4.19)$$

The energy spectrum for different values of S both for small values of n and in the asymptotic limit are plotted and discussed in section 6.

4.1.2. $\vec{n} \perp \mathbf{\Pi}$ For this ansatz, the components of $\mathbf{\Pi}$ are related to the *azimuthal* angle ϕ in the $x - y$ plane as:

$$\Pi_x = -\Pi \sin \phi; \quad \Pi_y = \Pi \cos \phi \quad (4.20)$$

so that the energy of the particle, given as :

$$E = n_x \Pi_y + n_y \Pi_x = 0 \quad (4.21)$$

However, with this choice of co-ordinate axis, the variation of the *polar* angle θ crosses singular points at poles. We choose a suitable co-ordinate frame to avoid the singular points. In the new frame the equations of motion are:

$$\begin{aligned} \dot{\Pi}_x &= -\cos(\theta); \quad \dot{\Pi}_y = \sin(\theta) \sin(\phi) \\ \dot{\theta} &= \Pi_x; \quad \dot{\phi} = \Pi_y - \Pi_x \frac{\cos(\theta)}{\sin(\theta)} \sin(\phi) \end{aligned} \quad (4.22)$$

In the $z - x$ plane ($\theta = \pi/2$) the above equations simplifies to:

$$\dot{\Pi} = \sin(\phi); \quad \dot{\phi} = \Pi \quad (4.23)$$

where $\Pi = \Pi_y$. Combining the above equations we get,

$$\ddot{\phi} + \sin(\phi) = 0 \quad (4.24)$$

which maps to the pendulum equation. ϕ maps to the angular co-ordinate or the amplitude, Π to the momentum and $\cos \phi$ to the potential energy of the pendulum. The angular momentum

$$\frac{J_z}{S} = \cos \phi + \frac{\Pi^2}{2} \quad (4.25)$$

maps to the total energy $\cos \phi + \frac{\phi^2}{2}$ of the pendulum which is a conserved quantity. The general solution to eqn.(4.24) is Legendre's elliptic function of the first kind. Π can also be subsequently computed from the values of ϕ after subsequent substitution in eqn (4.23).

For $J_z < S$ the particle will execute *libration*. This involves a back-and-forth motion in real space and the phase space motion is contractable to a point in topological sense. The geometrical phase for this motion is zero. For $J_z > S$ the particle will undergo complete *rotations* in the $z - x$ plane. The geometric phase picked up during one complete *rotation* is 2π . Since, $\Pi_x = 0$, the Bohr-Sommerfeld quantization condition for $J_z > S$ is:

$$\Omega = 2\pi \frac{m}{S} \Rightarrow S = m \quad (4.26)$$

where m is an integer.

The zero energy modes for the regime $J_z < S$ occurs both for the integer and half integer S . However as the J_z value increases and $J_z > S$, the above Bohr-Sommerfeld quantization condition dictates that the zero modes, will appear only for the integer spins.

To summarize, the semiclassical analysis predicts that there will be a zero energy state for every value of J_z for integer S but for half odd-integer S , they will be zero energy states only for $J_z < S$.

4.2. Quantum spectrum

In this section, we study the quantum mechanical spectrum of the system in a constant external magnetic field B . In the dimensionless units defined earlier, the hamiltonian for the system is:

$$\mathcal{H} = \frac{1}{S} \mathbf{S} \cdot \mathbf{\Pi} \quad (4.27)$$

with $[\Pi_i, \Pi_j] = \epsilon_{ij}$. We define the operators a and a^\dagger as,

$$a = \frac{1}{\sqrt{2}} (\Pi_x - i\Pi_y) \quad (4.28)$$

$$a^\dagger = \frac{1}{\sqrt{2}} (\Pi_x + i\Pi_y) \quad (4.29)$$

they satisfy the commutation relation $[a, a^\dagger] = 1$. With the standard notation, $S^\pm = S_x \pm iS_y$, the hamiltonian is:

$$\mathcal{H} = \frac{1}{S\sqrt{2}} (S^- a^\dagger + S^+ a) \quad (4.30)$$

For $S = 1/2$ our model maps on to the strong coupling limit of Jaynes-Cummings model[12]. For general S , the model maps to the strong coupling limit of the Tavis-Cummings model [19, 20].

The Tavis-Cummings model is exactly solved using the Bethe ansatz. However, we can deduce several qualitative features of the spectrum from the symmetry properties alone. The hamiltonian is rotationally invariant. The generator of rotations is,

$$J_z = a^\dagger a + S_z \quad (4.31)$$

J_z commutes with the hamiltonian and hence in the basis of the eigenstates of J_z , the hamiltonian will be block diagonal. The eigenstates of J_z can be constructed as follows. Let

$$a^\dagger a |n, m\rangle = |n, m\rangle, \quad n = 0, 1, \dots \quad (4.32)$$

$$S_z |n, m\rangle = m |n, m\rangle, \quad m = -S, \dots, S \quad (4.33)$$

we then have,

$$J_z |n - k, -S + k\rangle = j |n - k, -S + k\rangle, \quad j \equiv n - S \quad (4.34)$$

For $-S \leq j \leq S$, there are $n + 1$ ($= J + S + 1$) values of k and thus the corresponding blocks of the hamiltonian will be $J + S + 1$ dimensional. For $J \geq S$ the dimension of the blocks is $2S + 1$.

For all values of S , there is an operator $\Sigma \equiv e^{i\pi S_z}$ which anti-commutes with the hamiltonian. This implies that the eigenvalues of \mathcal{H} have to come in pairs, namely if ϵ is an eigenvalue then $-\epsilon$ is also an eigenvalue. Σ commutes with J_z and hence the eigenvalues of each block will have to come in pairs. Thus every block with odd dimension has to have at least one zero eigenvalue.

The lowest value of j is $j = -S$. There is only one state in this block, $|0, -S\rangle$. It is easy to verify that this is always an zero energy eigenstate of \mathcal{H} . Thus the blocks $j = -S + 2n$ will all have atleast one zero eigenvalue for $2n < S$. For $j \geq S$, the dimension of the blocks, as mentioned earlier, is $2S + 1$. Thus for integer S , there is atleast one zero eigenvalue in each such block. For half-odd integer S , this is not necessary.

The hamiltonian can also be diagonalised analytically in the $j \gg S$ limit. In this limit, the hamiltonian reduces to

$$H = \frac{\sqrt{2n}}{S} S^y (1 + o(1/n)) \quad (4.35)$$

where $n = J + S$. The energy eigenvalues of the $2S + 1$ branches, in this limit are therefore,

$$E = \sqrt{2n} \frac{m}{S}, \quad m = -S, \dots, S \quad (4.36)$$

The energy eigenvalues can be numerically computed for low values of n . We have shown the spectrum for $S = \frac{1}{2}, 1$ and $S = \frac{9}{2}, 5$ in figure [1].

5. Discussion

We now compare the results of the semiclassical quantization and the exact spectrum. In the free particle case the two spectra agree exactly. There is no exact match of the spectrum in a constant magnetic field and comparison is more interesting.

We first consider the zero-energy states. The semi-classical analysis predicts that zero energy modes will occur for $j < S$. This is consistent with the results obtained from the exact analysis. The quantum spectrum has zero modes only the odd dimensional subspaces. This detail is not reproduced by the semiclassical analysis. However, we note that that the semiclassical regime in our formalism is the opposite limit, $j > S$. In this regime the semiclassical analysis predicts zero modes only for integer S and that is indeed borne out by the exact spectrum.

The exact spectrum has $2S + 1$ branches for every $j > S$. However, we have only two branches of classical solutions. So which branch does it correspond to ? A comparison of the asymptotic results for the exact and the semiclassical asymptotic analysis, equations (4.36) and (4.19) shows that the classical solutions correspond to $m = \pm\sqrt{S}$. Namely, should lie between $\pm m$ and $\pm(m + 1)$ where $m < \sqrt{S} < m + 1$. Our numerical computations plotted in figure 1 shows that this is true even for small values of S . For $S = 1/2$, while the $\sqrt{2n}$ dependence of the spectrum is reproduced, the semiclassical spectrum overestimates the energies by a factor $\approx \sqrt{2}$.

6. Results and conclusions

To summarize our results, the semiclassical spectrum obtained by Bohr-Sommerfeld quantization reproduces the exact quantum spectrum for the case of a free particle on a cylinder.

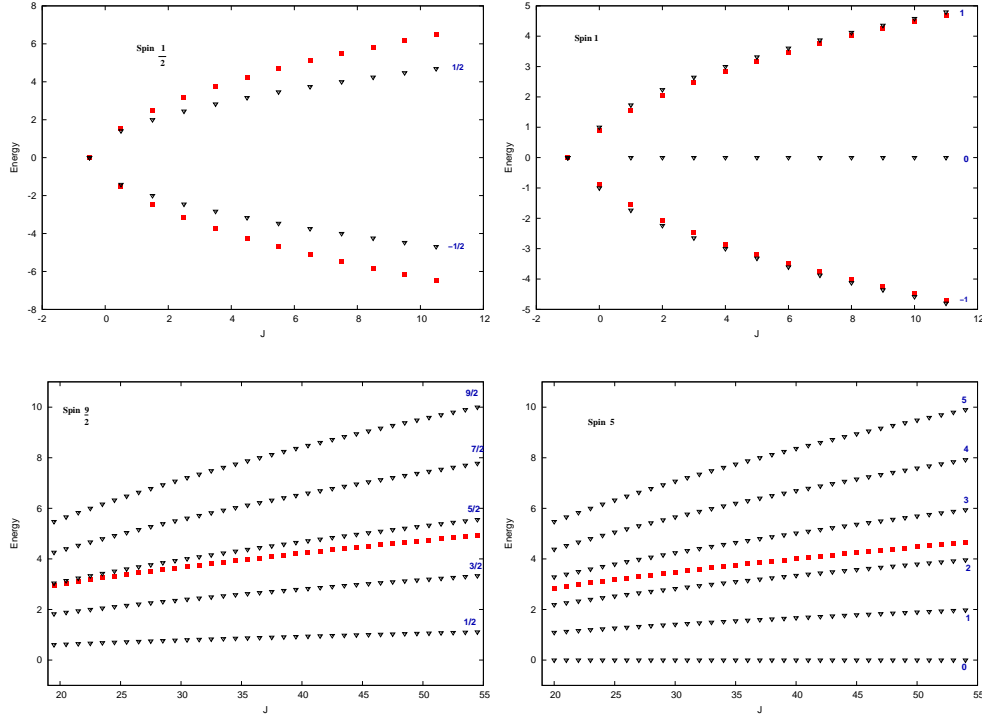


Figure 1: (Color online) Plots showing the energy spectrum obtained from semi-classical analysis and the exact quantum spectrum. The curves with red square points are obtained from semi-classical analysis. The quantum spectrum is denoted by black triangles. Figs. (1a),(1b), (1c),(1d) are the plots for $S = 1/2, 1, 9/2$ and 5 respectively. For the quantum spectrum, the energy branches corresponding to the different S_z values for a given S are marked. To avoid clutter only the positive energy branches of the spectrum for high S values are plotted. In the large n limit, the semi-classical spectrum gives the $\sqrt{S} - \hbar$ branch of the quantum spectrum.

For the particle in a constant magnetic field, the semiclassical spectrum correctly predicts the occurrence of zero energy branches for integer S and their absence for half-odd integer S for $j > S$. The exact solutions have $2S + 1$ branches in this regime. The classical solutions we have found yields a average of these branches. We note that the level spacing between these branches is $\sim S^0$. Hence more detailed quantitative agreement may be obtained by doing the gaussian fluctuations about the classical solutions instead of Bohr-Sommerfeld quantization.

We thank M.V.N. Murthy, Matthias Brack, Diptiman Sen and Bindu Bambah for useful discussions. M.M thanks M. Deha for discussions related to the numerical computation.

References

- [1] Novoselov K S, Geim A K , Morozov S V, Jiang D , Zhang Y , Dubonos S V, Grigorieva I V, and Firsov A A 2004 *Science*, **306**, 666; Novoselov K S, Geim A K, Morozov S V, Jiang D,

- Katsnelson M I, Grigorieva I V, Dubonos S V, and Firsov A A 2005 , *Nature*, **438**, 197; Zhang Y, Tan Y W, Stormer H L and Kim P 2005 *Nature*, **438**, 201.
- [2] Bernevig B A and Zhang S C 2006 *Phys. Rev. Lett.* **96**, 106802; Bernevig B A, Hughes T L and Zhang S C 2006 *Science* **314**, 1757; König M, Wiedmann S, Brüne C, Roth A, Buhmann H, Molenkamp L W, Qi X L and Zhang S C 2007 *Science* **318**, 766; Hassan M Z and Kane C L 2010 *Rev. Mod. Phys.* **82**, 3045 and the references therein.
- [3] Fu L and Kane C L 2008 *Phys. Rev. Lett.*, **100**, 096407; Akhmerov A R, Nilsson J and Beenakker C W J 2009 *Phys. Rev. Lett.*, **102**, 216404; Tanaka Y, Yokoyama T and Nagaosa N 2009 *Phys. Rev. Lett.*, **103**, 107002.
- [4] Mondal S, Sen D, Sengupta K and Shankar R 2010 *Phys. Rev. Lett.*, **104**, 046403, Mondal S, Sen D, Sengupta K and Shankar R 2010 *Phys. Rev. B*, **82**, 045120.
- [5] Zülicke U, Bolte J and Winkler R 2007 *New Journal of Physics*, **9** 355.
- [6] Rusin T M and Zawadzki W 2008 *Phys. Rev. B*, **78**, 125419.
- [7] Zawadzki W 2011 *J. Phys.: Condens. Matter*, **23**, 143201.
- [8] Yip P 1983 *J. Math. Phys.*, **24**, 1206.
- [9] Chen Y L, Analytis J G, Chu J H, Liu Z K, Mo S K, Qi X L, Zhang H J, Lu D H, Dai X, Fang Z, Zhang S C, Fisher I R, Hussain Z, Shen Z X and Shen Z X 2009 *Science* **325**, 178; Xia Y, Qian D, Hsieh D, Wray L, Pal A, Lin H, Bansil A, Grauer D, Hor Y S, Cava R J and Hasan M Z 2009 *Nature Phys.* **5**, 398.
- [10] Pauli W 1932 *Helv. Phys. Acta* **5**, 179.
- [11] Broglie L de, *La Théorie des Particules de Spin 1/2* (Gauthier-Villars, Paris, 1952).
- [12] Rubinow S I and Keller J B 1963 *Phys. Rev.* **1**, 2789.
- [13] Yabana K and Horuichi H 1987 *Prog. Theor. Phys.* **77**, 517.
- [14] Kuratsuji H and Iida S 1985 *Prog. Theor. Phys.* **74**, 439.
- [15] Kuratsuji H and Iida S 1988 *Phys. Rev. D* **37**, 441.
- [16] Bolte J and Keppeler S 1998 *Phys. Rev. Lett.* **81**, 1987 ; Bolte J and Keppeler S 1999 *Ann. Phys.*, NY **274**, 125.
- [17] Pletyukhov M and Zaitsev O 2003 *J. Phys. A: Math. Gen.* **36**, 5181.
- [18] Pletyukhov M, Amann C, Mehta M and Brack M 2002 *Phys. Rev. Lett.* **89**, 116601.
- [19] Bogoliubov N M, Bullough R K and Timonen J 1996 *J. Phys. A: Math. Gen.*, **29** 6305 .
- [20] Lee Y H, Links J and Zhang Y Z 2011 *Nonlinearity*, **24**, 1975 .